Investigation of the negative space charge layer by particle-in-cell simulation

Dan Wang, Lijun Wang, Jie Liu, Rui Wang, Chao Yan

State Key Laboratory of Electrical Insulation and Power Equipment, Xi'an Jiaotong University, Xi'an, China

Abstract: In this paper, the negative space charge layer formation and development at the streamer front is studied using a particle model. Simulations are performed in nitrogen under a pulsed voltage. Results show that a negative space charge layer is clearly distinguished at the streamer front. During the streamer propagation, the thickness of the space charge layer decreases, and the position corresponding to the peak value in the electron energy distribution shifts toward low energy.

Keywords: streamer, the space charge layer, particle simulation.

1. Introduction

Since Raether[1], Loeb and Meek[2] first reported on the streamer mechanism, the subject has received increasing attention. Positive streamers can emerge at a lower voltage, so they are easily to generate in experiments and have attracted more attention[3]. Negative streamers also widely exist in nature and industry, for examples, C-GIS and trigatrons[4], so studies on negative streamers are valuable. Negative streamers can initiate from several seed electrons. During the propagation of electron avalanches, electrons are accelerated efficiently and accumulate at the front, while ions are left behind. As a result, a negative space charge layer at the streamer head and a cathode sheath at the streamer tail form as shown in Fig. 1.

The space charge layer plays an important role during the streamer propagation. In our recent work[5], the simulation results suggested that the non-homogeneous distribution of energetic electrons at the negative streamer head is probably the primary mechanism responsible for the negative streamer branching. Therefore, a deep understanding of the space charge layer formation and development in negative streamers is very important and necessary. In Ref. 6, the authors developed a one dimensional fluid model in local field approximation to investigate the negative streamer ionization front and compared results with those from particle models. The physical discrepancies between results from the particle model and their fluid model lay in the leading edge of the front. Though the effect was not so much seen in the velocity, but much more in the ionization level behind the front. In Ref. 7, a high order fluid model was developed and used to study the propagation of negative fronts in nitrogen. Electron density, electric field, average energy and propagation velocity were given by this high order fluid model. In Ref. 8, a hybrid coupling was developed for the streamer pulled front. The authors coupled the extended fluid model with the particle model to reduce the calculation as well as provide generic features of streamer fronts. In Ref. 9, the particle model was applied to reproduce the ionization front formation and development in argon and nitrogen. The detailed structure including the kinetic front, the interior and the tail of the negative streamer was shown. However, in Ref. 9, the rotational excitation between electrons and nitrogen molecules was not considered, which resulted that the streamer propagated faster in nitrogen than argon.

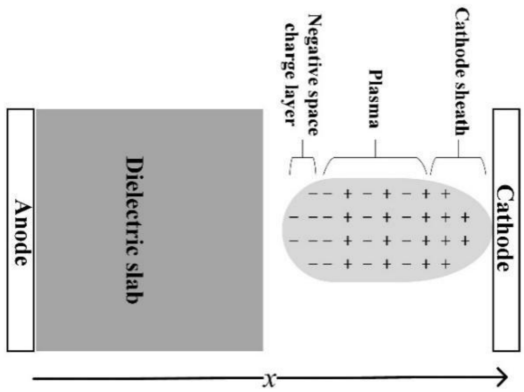

Fig. 1. The schematic diagram of the simulation physical model.

While the space charge layer can also be obtained with fluid models, in consideration of some non-equilibrium features, a detailed particle model is needed. In spite of many studies on the streamer, detailed studies concentrated on the space charge layer formation and development are still limited. So in this paper, a one dimensional (1D) particle-in-cell/Monte Carlo collisional (PIC/MCC) model is developed, and a detailed process of the space charge layer formation and development during the negative streamer propagation in nitrogen is given. The rotational excitation between electrons and nitrogen molecules is included in the simulations. The study can give a qualitative understanding of the space charge layer, lay the groundwork for the two dimensional or complete three dimensional simulations in the future and provide a reference for the industrial applications.

2. Simulation model

Following the configuration chosen in Ref. 9, the similar configuration used in this study includes two parallel planar electrodes, a gas gap and a dielectric slab to avoid the transition to the arc. As shown in Fig. 1, the anode grounded is located at $x = 0$, and the cathode with a nanosecond pulsed voltage is located at $x = 1$ cm. The length of the gas gap is 5 mm. The nanosecond pulsed voltage applied to the cathode has a rise time of 10 ns. A typical voltage with amplitude of 100 kV is plotted in Fig. 2.

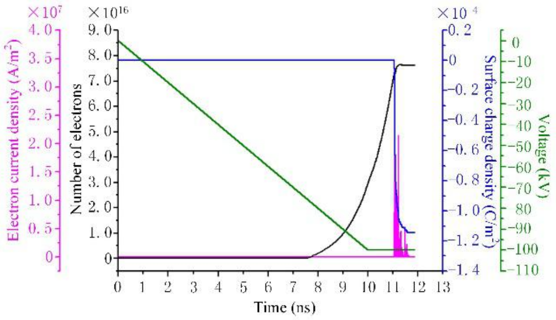

Fig. 2. The voltage, the number of electrons in the calculation domain, the electron current density and the charge density on the dielectric slab surface as the function of time.

The PIC/MCC model in this paper considers one dimension in space and three components of velocity. Using the VSim code which has been benchmarked in some works[10-12], the instantaneous position of charged particles is solved by the Newton's law; the Poisson equation for the electric field is solved in 1D Cartesian coordinates; collisions are processed with the Monte Carlo technique. To obtain a stable and reliable solution, we use the grid length $\Delta x = 2\times10^{-6}$ m and time step $\Delta t = 1\times10^{-13}$ s. Simulations in this paper are performed in nitrogen. At the beginning of the simulation, 100 macro electrons representing 100 physical electrons (the weight of the macro electron is 1) are placed near the cathode. Collisions between electrons and nitrogen molecules include one elastic scattering collision[13], one electron impact ionization collision[13], one rotational excitation collision[14], 15 vibrational excitation collisions[13] and 29 electronic excitation collisions[13]. Momentum exchange and charge exchange between ions and molecules are also included. For all collisions, it is assumed that the energy and the density of the background gas are not changed. The gas in the simulation is pure nitrogen, electron sources in the gas like electron detachment from ions and photoionization are not considered in our model.

3. The negative space charge layer formation and development

In the simulation, the background gas is nitrogen; the gas density is 2.5×10^{25} m^{-3}; the gas temperature is 300 K; and the voltage amplitude applied on the cathode is 100 kV. The time evolution of the applied voltage, the number of electrons in the calculation domain, the electron density and the surface charge density deposited on the dielectric slab is shown in Fig. 2. It can be seen that the increasing rate of electron number changes at about 7.5 ns. As investigated in Ref. 15, the change of the electron increasing rate indicates the transition in the discharge from the avalanche regime to the space charge affected regime. So 7.5 ns can be regarded as the time when the negative space charge layer at the streamer front forms in this simulation.

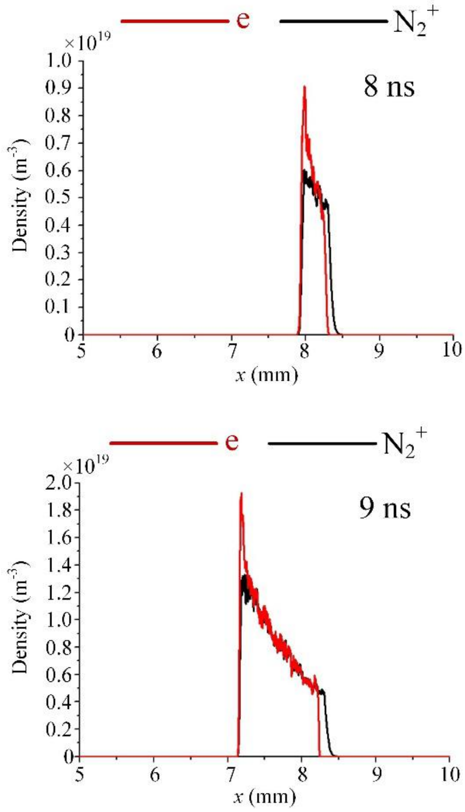

Fig. 3. The density of electrons and ions.

Fig. 3 shows the density of electrons and ions at different times. At 8 ns, the maximum density of electrons in the streamer front comes up to 9×10^{18} m^{-3}, while the ion density is obviously lower than the electron density. As a result, a noticeable negative space charge layer forms at the streamer head. At 8 ns, the thickness of the negative space charge layer is about 3 mm, while at 9 ns, the negative space charge layer is about 1 mm. During the development of the space charge layer, the thickness decreases.

Fig. 4 shows the distributions of the electron velocity and the ion velocity in x-direction. At 8 ns, the electron velocity in the negative streamer front is up to 3×10^{6} m/s, while it is below 1×10^{6} m/s in the plasma. The increase of the velocity in the streamer front is resulted from the electric field enhanced by the negative space charge at the streamer front. It also can be seen that besides the streamer front, the electron velocity in the cathode sheath is also enhanced. This phenomenon can be explained by the distorted electric field resulted from the positive space charge in the cathode sheath. However, at the next moment, the electrons in the cathode sheath are accelerated into the plasma, and the velocity decreases at 9 ns. It should be noted that velocities in positive x-direction and opposite x-direction are not equilibrium for both electrons and ions because electrons at the streamer front are accelerated toward the anode, while ions in the cathode sheath are accelerated toward the cathode.

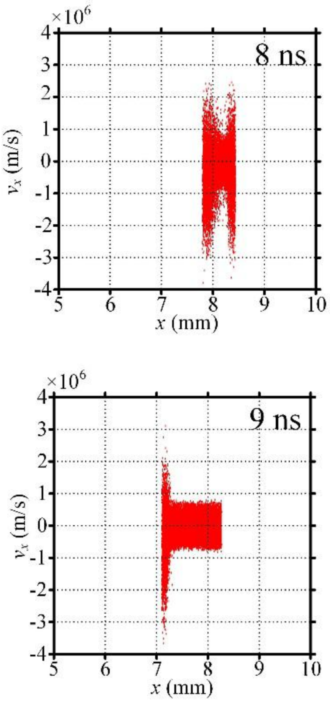

Fig. 4. The distribution of electron velocity in x-direction.

The average energy distributions of electrons and ions along x-axis at different times are shown in Fig. 5 and Fig. 6 respectively. In Fig. 5, it can be seen that the electron energy in the streamer front is significantly higher than that in the streamer body. The average electron energy in the negative space charge layer at the streamer front is up to 17.5 eV, while it is about 2 eV in the plasma, which indicates that the ionization mainly takes place in the space charge layer. The electrons with energy above ionization threshold in the space charge layer ionize the background nitrogen molecules and generate plasma, which can explain the phenomenon that the thickness of the space charge layer at the streamer front decreases, and the length of the plasma increases as observed in Fig. 3. In the plasma, the average electron energy is low. The reasons for this is two-folds. On the one hand, the electric field in the plasma is screened out so that cannot accelerate the electrons in the plasma efficiently; on the other hand, the electrons with low energy will lose their energy quickly because of a variety of impact excitation processes. As shown in Fig. 6, ions are slightly accelerated at the streamer front but significantly accelerated in the cathode sheath especially when the streamer arrives at the dielectric slab. At 12 ns, the negative space charge layer disappears, and there is a good conductivity in the plasma, therefore the high voltage applied on the gap is almost applied on the cathode sheath. As a result, the ions in the cathode sheath are accelerated rapidly, and electrons in this sheath are expelled quickly. So the ion energy in the cathode sheath increases significantly, and the cathode sheath expands slightly as shown in Fig. 6.

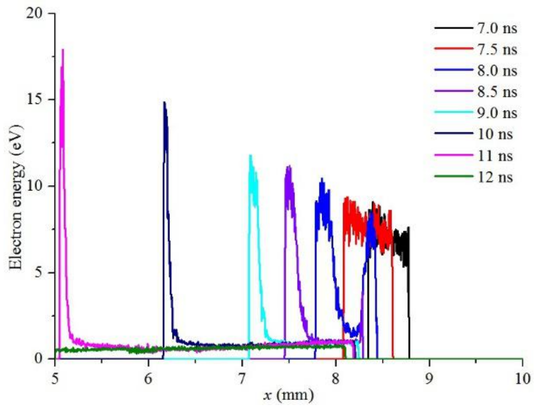

Fig. 5. The distributions of the average electron energy along x-axis.

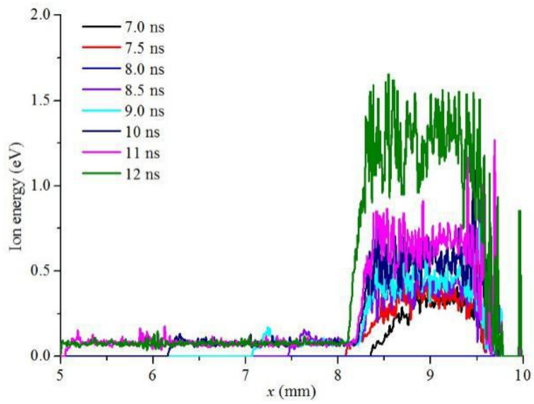

Fig. 6. The distributions of the average ion energy along x-axis.

The electron energy distributions at different times are plotted in Fig. 7. At 7 ns, the time before the space charge layer forms, the electron distribution among different energy levels are uniform. After 7 ns, the proportion of electrons with low energy increases with time, which is resulted from the increase of electrons in the plasma. It should be noted that the peak positions where the peak values correspond are in the range of 0-3 eV. This feature can be explained by the vibrational and rotational excitations in nitrogen. Compared with electronic excitations, excitation thresholds are lower, and cross sections are larger in rotational and vibrational excitations. So the rotational and vibrational excitations are the dominant collisions in the plasma. Note that thresholds of rotational and most vibrational excitations in nitrogen are below 3 eV. When the electrons are accelerated to the thresholds, they will have possibility of losing a part of energy to excite the molecules. As a result, most of electrons are of energy below 3 eV. And because of the screening of the field in the plasma, they cannot be accelerated efficiently so that their energy decreases further as time goes by, which can explain that the peak value corresponding position shifts toward low energy as shown in Fig. 7.

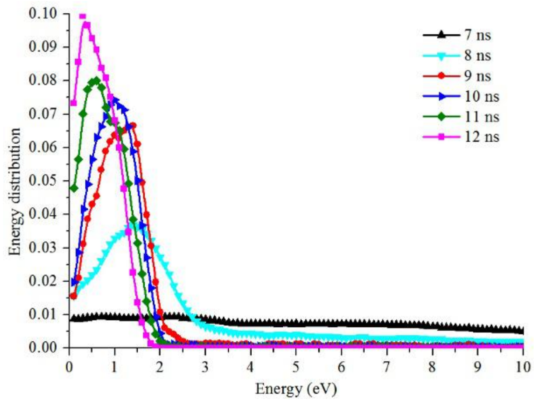

Fig. 7. The electron energy distributions.

4. Conclusion

The space charge layer formation and development under a pulsed voltage has been studied using a 1D PIC/MCC model. A complete negative streamer structure including the negative space charge layer, the plasma body and the cathode sheath has been presented. The streamer density, the charged particle velocity and energy distributions have been obtained. Some significant phenomena have been observed and analyzed. During the negative streamer formation and propagation, a negative space charge layer forms at the streamer front. In this space charge layer, the electron energy is much higher than the plasma body. As the space charge layer develops, the electron energy increases while the thickness decreases. The position corresponding to the peak value in the electron energy distribution shifts toward low energy, which is resulted from the increase of the plasma where the electric field is screened out, and electrons lose their energy quickly by excitation collisions.

5. References

[1] H. Raether, Zeitschrift Für Physik 112, 464-489 (1939).

[2] L. B. Loeb and J. M. Meek, Journal of Applied Physics 11, 459 (1940).

[3] A. Luque, V. Ratushnaya, and U. Ebert, Journal of Physics D: Applied Physics 41, 234005 (2008).

[4] L. Wang, X. Huang, S. Jia, Y. Liu, S. Shang, and T. Du, IEEE Transactions on Plasma Science, 42, 1393-1399 (2014).

[5] D. Wang, L. Wang, and Y. Zheng, Journal of Applied Physics 124, 203301 (2018).

[6] C. Li, W. J. M. Brok, U. Ebert, and J. J. A. M. van der Mullen, Journal of Applied Physics 101, 123305 (2007).

[7] A. H. Markosyan, S. Dujko, and U. Ebert, Journal of Physics D: Applied Physics 46, 475203 (2013).

[8] C. Li, U. Ebert, and W. Hundsdorfer, Journal of Computational Physics 229, 200-220 (2010).

[9] F. Taccogna and F. Pellegrini, Journal of Physics D: Applied Physics 51, 064001 (2018).

[10] P. Messmer and D. L. Bruhwiler, Computer Physics Communications 164, 118 (2004).

[11] K. Tian, H. Wang, F. Marhauser, G. Cheng, and C. Zhou, in Proceedings of PAC09, Vancouver, BC, Canada, TH5PFP093, 2009.

[12] C. Nieter, C. Roark, P. Stoltz, and K. Tian, in Proceedings of PAC09, Vancouver, BC, Canada, FR5PFP085, 2009.

[13] See http://www.lxcat.net for more information on Biagi database (last accessed on July 3, 2018).

[14] See http://www.lxcat.net for more information on Phelps database (last accessed on July 3, 2018).

[15] M. Rabie and C.M. Franck, Journal of Physics D: Applied Physics 49, 175202 (2016).